applied sciences

MDPI

Article

Influence of the Precipitation of Secondary Phase on the Thermal Diffusivity Change of Al-Mg_2Si Alloys

Yu-Mi Kim [1], Se-Weon Choi [1,*], Young-Chan Kim [1], Chang-Seok Kang [1] and Sung-Kil Hong [2,*]

[1] EV Components & Materials R&D Group, Korea Institute of Industrial Technology, 6 Cheomdan-gwagiro 208-gil, Buk-gu, Gwangju 61012, Korea; qpt146@kitech.re.kr (Y.-M.K.); kim0chan@kitech.re.kr (Y.-C.K.); cskang7@kitech.re.kr (C.-S.K.)

[2] School of Materials Science & Engineering, Chonnam National University, 77 Yongbong-ro, Buk-gu, Gwangju 61186, Korea

* Correspondence: choisw@kitech.re.kr (S.-W.C.); skhong@jnu.ac.kr (S.-K.H.); Tel.: +82-62-600-6330 (S.-W.C.); Fax: +82-62-600-6149 (S.-W.C.)

Received: 13 September 2018; Accepted: 20 October 2018; Published: 24 October 2018

Abstract: Al-Si-Mg alloys are investigated to determine the relationship between changes in the thermal diffusivity and precipitation behavior of the Mg_2Si phase with various contents of Mg_2Si and aging treatment conditions. The samples were solid solution-treated and then quenched with water (80 °C). Aging treatments were implemented at temperatures ranging from 180 to 240 °C for 5 h. The precipitation behavior of Mg_2Si was observed using a heat flow curve using differential scanning calorimetry analysis. The thermal diffusivity of Al-Mg_2Si alloy was affected by the precipitation of the Mg_2Si phase, particularly in the meta-stable β phase. In the temperature range of precipitation occurrence, the thermal diffusivity of the alloy increased with the temperature when the precipitation of the meta-stable β phase of the sample was incomplete. However, at the same temperature, the samples in which precipitation had completed did not have any increased thermal diffusivity. The thermal diffusivity of the samples decreased when the meta-stable Mg_2Si phase had dissolved in the matrix. The precipitation and dissolution of Mg_2Si mainly affected the variation of thermal diffusivity in Al-Si-Mg. In contrast, the stable Mg_2Si phase was not affected by changes in thermal diffusivity at a high temperature.

Keywords: aluminum casting alloy; heat treatment; laser flash method; thermal diffusivity; Mg_2Si

1. Introduction

Since electric appliances have gradually become smaller and are now packaged with additional features including complex specifications, the operating temperature has become an important issue. Heat in an electronic application reduces both the efficiency of the electronic device and its service life [1,2]. One of the cooling methods used for electronic applications is the heat sink attachment method. According to Fourier's law, the heat dissipation efficiency of a heat sink is proportional to the thermal conductivity of the heat sink material [3]. When the heat sink has thermal conductivity κ, Fourier's law is expressed as:

$$dq/dt = -\kappa A(dT/dx) \quad (1)$$

where κ is the thermal conductivity, dq/dt is the heat flow, A is the cross sectional area in the x direction, and dT/dx is the temperature difference in the +x direction. Therefore, using materials with high thermal conductivity, such as heat sink materials, is commonly recommended [1].

In response to the recent issues related to the reduced efficiency of electronic devices due to heat generation, many researchers have carried out studies aimed at identifying a high thermal conductivity material, as well as a method for measuring thermal conductivity [4–7]. Thermal diffusivity reflects

the actual specimen state, which includes not only the internal state but also the surface state [8,9]. Thermal conductivity (κ) is related to thermal diffusivity (α) in the following equation:

$$\kappa = \alpha \cdot \varrho \cdot Cp \quad (2)$$

where ϱ is the material density and Cp is the heat capacity. The heat capacity and material density are defined according to the composition of the material, because they are physical properties. Thermal diffusivity refers to the rate at which heat travels from a high temperature to a low temperature in a material with a temperature difference. Therefore, since physical and chemical changes to the heat transfer path affect thermal diffusivity [10], the thermal conductivity for a material can be determined from its thermal diffusivity.

Laser flash analysis (LFA) is a thermal diffusivity measurement method in which a shot laser pulse irradiates a single sample face, and then an infrared (IR) detector monitors the temperature increase of the opposite side of the sample; the thermal diffusivity is calculated from the temperature increase versus the time profile [7,10,11]. The advantage of the LFA method is that it can be used to investigate small or thin samples from below zero to high temperatures (approximately 2000 K). In addition, thermal diffusivity reflects the material state in terms of microstructure, precipitation, defects, etc., when measured with LFA.

Al-Mg-Si alloys are widely used as heat sink materials. The 6XXX alloys are particularly advantageous due to their medium strength, excellent formability, high thermal conductivity, and low cost [12–15]. Mg and Si are the major elements in the 6XXX series, and they exist in the form of the Mg_2Si phase in Al. The type of precipitation phase can be controlled according to the heat treatment, and the type of Mg_2Si phase can be used to determine the alloy properties. The precipitations of the Mg_2Si unstable phases improve the strengths of the alloys [13,16,17]; in particular, among the various Mg_2Si precipitation phases, the β′ phase contributes most to improving the strength.

Thermal diffusivity can also be improved by the precipitation of solute in a matrix [10,18,19]; however, few studies have been carried out on the types of Mg_2Si precipitates that contribute to thermal diffusivity. The aim of this paper is to study the effects of Mg_2Si content and phase precipitation on the thermal diffusivity of Al-Mg_2Si alloys. In addition, the measurements of as-quenched and aging-treated specimens are compared in terms of factors such as thermal diffusivity and heat flow. This study has been carried out for the purpose of determining the influence of Mg_2Si content and aging treatment on thermal diffusivity, and to apply the design of a high thermal conductivity alloy and its heat treatment condition.

2. Materials and Methods

The Al-Mg-Si alloys were produced using gravity casting with 99.8 wt.% commercial pure Al, a 98.5 wt.% Si pellet, and 99.9 wt.% pure Mg. The alloys were comprised of different Mg and Si contents, and their compositions are shown in Table 1; the composition of Al-1.1Mg_2Si alloys is located in the hypo-eutectic field on the Al-Mg_2Si phase diagram [20]. The Al-1.9Mg_2Si alloy was designed for the eutectic composition in the Al-Mg_2Si system. The Al-1.9Mg_2Si alloy is located in a hyper-eutectic field on the phase diagram. The chemical compositions of the alloys were investigated through spark emission spectroscopic analysis. Gas bubbling filtration treatment was performed at 750 °C for 15 min with high purity (99.9%) Ar gas in the melt. The melt was stabilized for 15 min prior to casting. The melt was then poured into a permanent mold which was preheated to 95 °C after stabilization.

Table 1. The chemical compositions of studied alloys.

Alloys	Al	Si	Mg	Fe	Mg_2Si
Al-1.1Mg_2Si	98.80	0.39	0.73	0.10	1.1
Al-1.9Mg_2Si	97.91	0.67	1.32	0.11	1.9
Al-3.5Mg_2Si	96.30	1.22	2.36	0.11	3.5

The samples were heat treated at 590 °C for 30 min in the solution treatment, then quenched in water (at approximately 80 °C) in order to form a supersaturated solid solution. The samples were then aged at different temperatures from 180 to 240 °C. In addition, Al-1.9Mg_2Si was aged at 340 °C so as to observe the Mg_2Si precipitate. The Mg_2Si precipitate was observed using an optical microscope (OM), a scanning electron microscope (SEM), and a transmission electron microscope (TEM) after the aging treatment.

Thermal diffusivity was measured using a laser flash apparatus (LFA 457, NETZSCH, Selb, Germany). The samples were cut to a diameter of 12.7 mm and a thickness of 2.5 mm for the thermal diffusivity measurements. The samples were coated using a carbon spray prior to analysis in order to prevent the laser from reflecting on the surfaces of the samples. The LFA test was performed at a temperature range from 25 to 500 °C five times.

A differential scanning calorimetry (DSC) device (DSC 404 F1, NETZSCH, Selb, Germany) was used to investigate the microscale phase transformation by heat treatment condition. The samples were cut into cylindrical shapes of 6 mm diameter and 1 mm thickness. The DSC analysis was performed at a temperature range from 20 to 530 °C at a rate of 10 °C/min in a 99.999% N_2 atmosphere. The gas flow was fixed at 50 mL/min and a pre-vacuum sequence was performed in order to prevent oxidation of the samples.

An X-ray diffraction (XRD) device (X'pert Pro, PANalytical, Amelo, The Netherlands) was used to investigate the diffraction pattern of as-quenched Al-1.9Mg_2Si; the sample was also analyzed after DSC measurement. The sample was then used to identify the dissolution and precipitation of the Mg_2Si phase in Al-Mg_2Si alloy. Cu Kα radiation was used to define the sample precipitates.

3. Results and Discussion

The casting structures of the Al-Mg_2Si alloys were observed using an optical microscope and are shown in Figure 1. A number of crystallized phases were observed with increased Mg_2Si content. One of the crystallization phases had a gray color and a needle shape, while another had a black color and a sphere shape in all of the specimens. In particular, the number of black phases increased with increasing Mg_2Si content. The eutectic phase was only observed in Al-3.5Mg_2Si. The black phase was defined in the Mg_2Si phase according to the component analysis. The gray needle phase was analyzed in the AlFeSi ternary intermetallic compound. This compound appears when Al contains Fe as an impurity. The AlFeSi phase was found in all of the specimens, as shown in Figure 1.

The microstructures of the as-quenched Al-Mg_2Si alloys are shown in Figure 2. The AlFeSi phase was present in all of the as-quenched samples. However, the eutectic Mg_2Si phase only appeared in the Al-3.5Mg_2Si sample with a sphere shape that was larger than the as-cast sample. The Mg_2Si contents of the Al-1.1Mg_2Si and Al-1.9Mg_2Si alloys were similar to or lower than the solubility of Mg_2Si in the Al matrix at 590 °C. Therefore, the Mg_2Si phase of both samples was resolved during the solid solution treatment and could not be determined, and as such are not shown in Figure 2a,b.

The as-quenched Al-Mg_2Si samples were investigated using DSC to identify the phase transformation of the Mg_2Si, and their heat flow curves are shown in Figure 3. The heat flow curves have several exothermic peaks, and were named exothermic peaks, A, B, and C. The positions of the exothermic and endothermic peaks are at similar temperatures to those presented in previous studies [13,20,21]. For the Al-Mg_2Si pseudo-binary system, the Mg_2Si phase was precipitated as follows [22–24]: SSS $\rightarrow$ G.P. zone $\rightarrow$ β'' coherent precipitates $\rightarrow$ β' semi-coherent precipitates $\rightarrow$ β (Mg_2Si) incoherent precipitates. When compared with earlier studies, peaks A and B are composite peaks and seem to be related to the precipitations of β'' and β', respectively, while peak C is the result of the precipitation of the β phase.

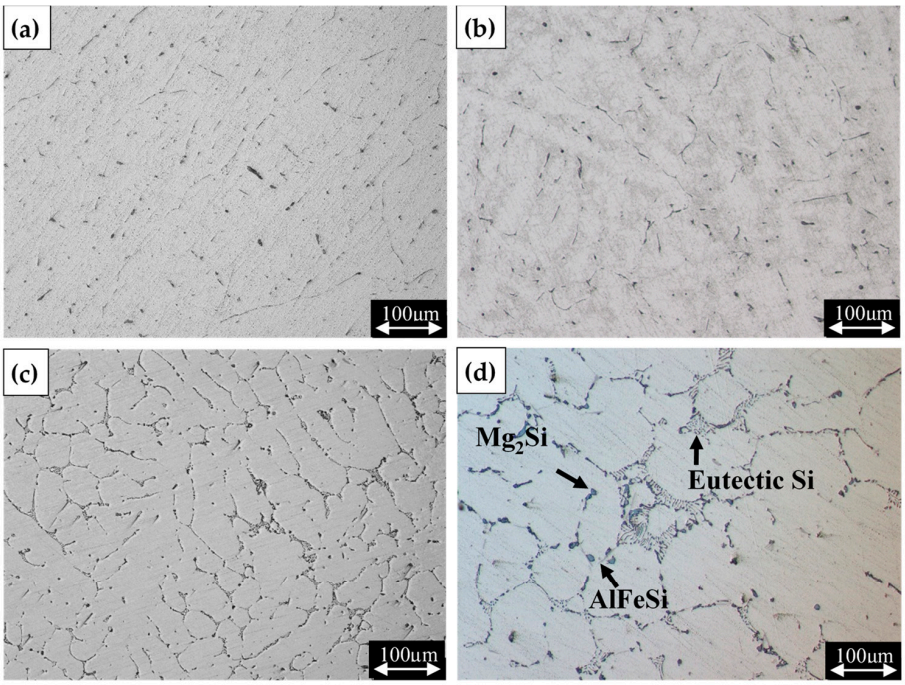

(e) Result of EDX analysis of Mg_2Si

Element	Wt.%	At.%
Mg	65	62
Si	35	38

Figure 1. Optical micrographs of as-cast Al-Mg_2Si alloys: (**a**) Al-1.1Mg_2Si; (**b**) Al-1.9Mg_2Si; (**c**) Al-3.5Mg_2Si; (**d**) high magnification of Al-3.5Mg_2Si (×500); and (**e**) result of energy dispersive X-ray spectroscopy (EDX) analysis of Mg_2Si phase (black phase in (**d**)).

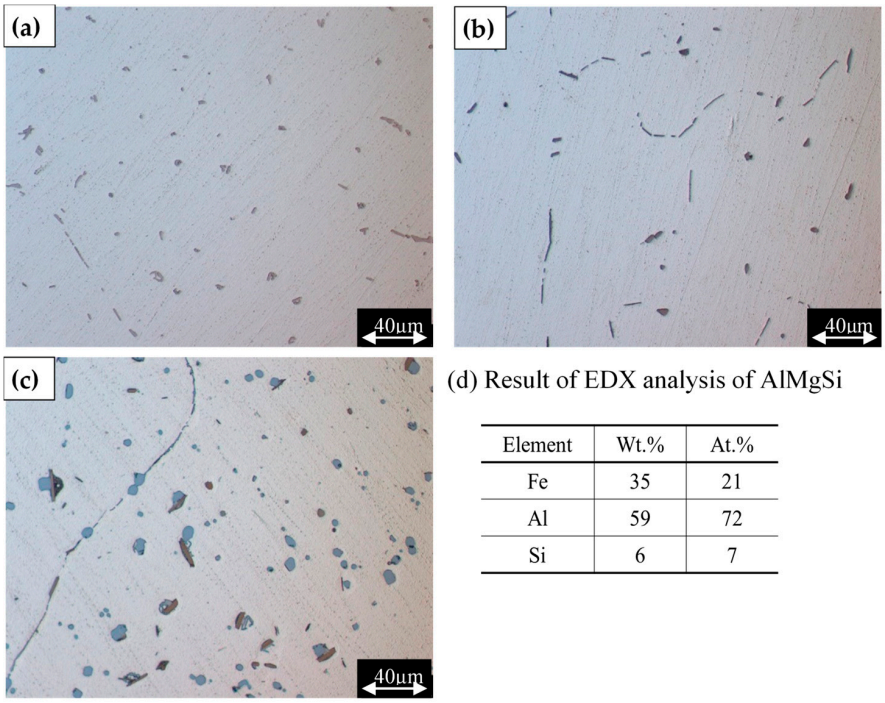

(d) Result of EDX analysis of AlMgSi

Element	Wt.%	At.%
Fe	35	21
Al	59	72
Si	6	7

Figure 2. Optical micrographs of as-quenched Al-Mg2Si alloys: (**a**) Al-1.1Mg2Si; (**b**) Al-1.9Mg2Si; (**c**) Al-3.5Mg2Si; and (**d**) result of EDX analysis of AlFeSi phase (gray phase in (**c**)).

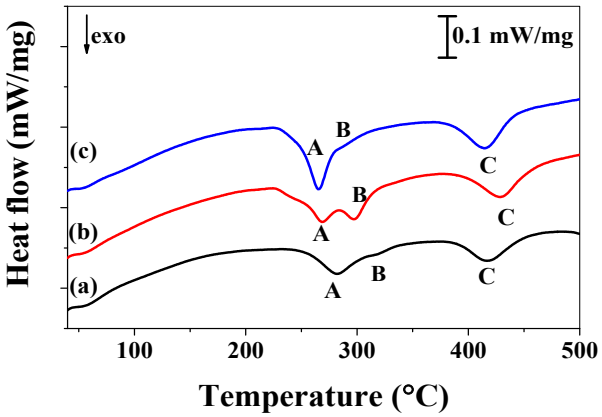

Figure 3. The heat flow curves of solid solution-treated samples according to temperature increases after quenching: (**a**) Al-1.1Mg2Si, (**b**) Al-1.9Mg2Si, and (**c**) Al-3.5Mg2Si.

The Al-1.9Mg_2Si samples were investigated using XRD to identify the presence of the Mg_2Si phase before and after the DSC analysis. In Figure 4a, the diffraction pattern of the as-quenched sample only has Al peaks. This is because the Mg and Si atoms were dissolved in the Al matrix during the solid solution treatment. However, according to the DSC analysis, the sample has the Al and Mg_2Si peaks in different diffraction patterns, as shown in Figure 4b. It can be determined from the Mg_2Si peaks that the Mg_2Si precipitation occurred during the DSC analysis sequence.

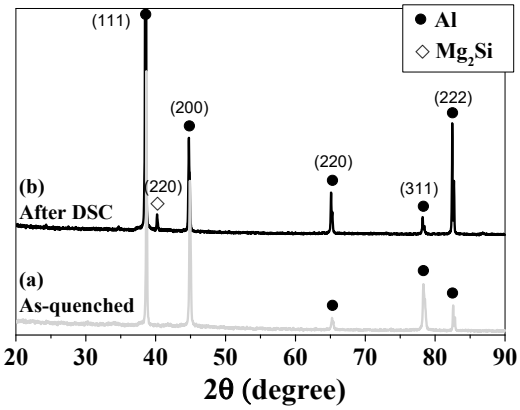

Figure 4. X-ray diffraction patterns of Al-1.9Mg2Si specimens: (**a**) as-quenched sample (supersaturated solid solution state) and (**b**) DSC analyzed sample.

The as-quenched Al-Mg_2Si samples were analyzed using LFA depending on the temperature, and the results are shown in Figure 5. The Al-1.1Mg_2Si alloy had the highest thermal diffusivity at every temperature. The Al-3.5Mg_2Si alloy had lower thermal diffusivity than the others. The thermal diffusivity gap between the Al-1.1Mg_2Si and Al-3.5Mg_2Si samples was measured as approximately 15 mm^2/s at 25 °C. This difference of thermal diffusivity between the two samples was attributed to two reasons: the content of the alloying element in alloys and the concentration of dissolved solute in the Al matrix after quenching. The additive atoms have a different size than the Al atoms. In general, the addition of alloying elements led to a decrease in thermal diffusivity. Further, if impurity atoms had dissolved in the Al matrix, those impure atoms caused a partial lattice distortion in the matrix; this distortion interrupted the movements of the heat carriers. Thus, thermal diffusivity decreased as the concentration of impurity atoms increased [16,20,21].

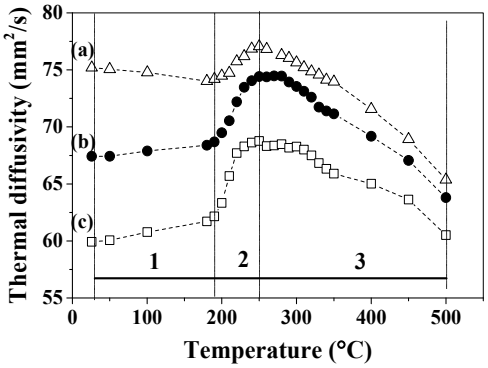

Figure 5. Thermal diffusivity changes of as-quenched samples according to increasing temperature: (**a**) Al-1.1Mg_2Si, (**b**) Al-1.9Mg_2Si, and (**c**) Al-3.5Mg_2Si.

In general, thermal diffusivity linearly decreased with the increase of temperature above room temperature. This was because the heat vibrations of the matrix atoms interrupted the movements of free electrons in the lattice [10]. However, in our study, the thermal diffusivity tendency of each specimen changed with temperature and content. In Figure 5a, the slope of the thermal diffusivity curve had a negative value at zone 1; however, the Al-3.5Mg_2Si specimen (Figure 5c) had a small positive slope in the same zone. Zone 1 was defined as the range in which thermal diffusivity was continuously and linearly changed corresponding to the increase of temperature. Zhang et al. [25] demonstrated that the co-cluster and the Guinier-Preston (GP) zone combined and precipitated at below 200 °C. This zone included the precipitation temperature of the GP zone. It appears that the precipitation of the solute affected the increase in thermal diffusivity.

The thermal diffusivities of the samples rapidly increased at a specific temperature range, as shown in Figure 5; this temperature range was called zone 2. The temperature of zone 2 matched the precipitation temperatures of the β″ and β′ phases (A and B peaks) in Figure 3. As the GP zone developed to the β″ and β′ phases, the precipitations of the β″ and β′ phases reduced the concentration of solute atoms in the Al matrix [10,26]. As a result, heat transfer was facilitated, and the thermal diffusivity increased [27]. The thermal diffusivity of the Al-3.5Mg_2Si specimen increased in zones 1 and 2, as shown in Figure 5c. Al-3.5Mg_2Si had the largest amount of dissolved solute in the matrix, and the precipitation of the dissolved solute contributed to the increased thermal diffusivity.

The thermal diffusivities of all of the samples decreased at temperatures above zone 2, as shown in Figure 5, due to the thermal vibration of the atoms in the matrix, which interrupted the heat transfer [28]. The heat energy excited the metal atoms and increased the temperature of the metal. The thermal vibration of the excited atoms interrupted the free electron transfer through the matrix [29]. Therefore, the thermal diffusivities of the specimens decreased with the increase of temperature in zone 3.

The as-quenched samples were aged at temperatures ranging from 180 to 240 °C for 5 h. The Al-1.9Mg_2Si specimens were analyzed with OM, SEM, and TEM, and the results of these analyses are shown in Figure 6. The precipitate cannot be observed using SEM, and as shown in Figure 6a, only the AlFeSi phase appeared. In Figure 6b, a small precipitate was present after the aging treatment at 180 °C for 5 h. The size of this small Mg_2Si phase (β″) was 30 nm. The particles were too small to be observed in the SEM image of Figure 6a. Precipitate was detected by the optical microscope after aging at 240 °C. The precipitate seems to be similar to the black dot in Figure 6c. The average size of the Mg_2Si was less than 1 μm with an aging temperature of 240 °C. In Figure 6d, a lot of Mg_2Si was randomly distributed on the Al matrix of 4–6 μm.

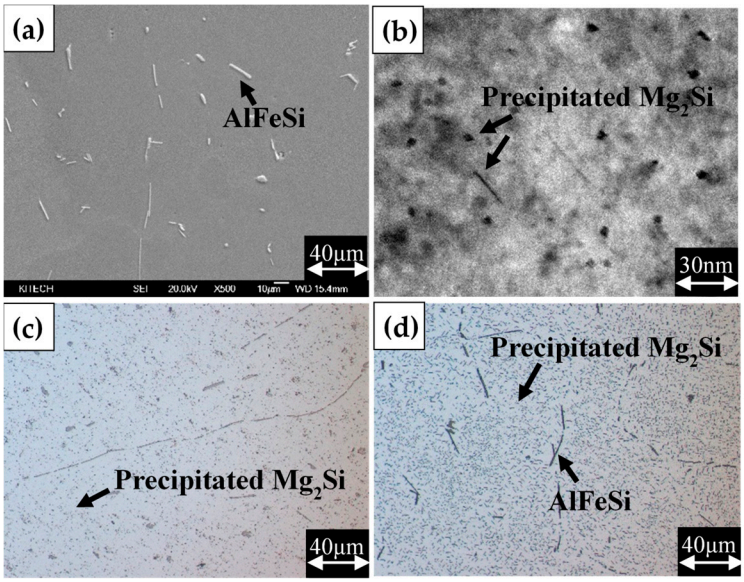

Figure 6. The precipitation of Mg_2Si phase in Al-1.9Mg_2Si alloy: (**a**) scanning electron microscope (SEM) photograph after aging treatment at 180 °C for 5 h; (**b**) transmission electron microscope (TEM) photograph after aging treatment at 180 °C for 5 h; (**c**) optical microscope (OM) photograph after aging treatment at 240 °C for 5 h; and (**d**) OM photograph after aging treatment at 340 °C for 5 h.

Aged Al-1.1Mg_2Si was also analyzed in terms of thermal diffusivity using LFA and the results are shown in Figure 7. Thermal diffusivity at 25 °C increased from 77 mm^2/s to 84 mm^2/s with the increase of the aging temperature from 180 to 240 °C. The thermal diffusivity of the Al-1.1Mg_2Si samples decreased with the increase of temperature in zone 1 (below 200 °C). In zone 2, the thermal diffusivity of the 180 °C aged sample increased with the increase of temperature. The increment of thermal diffusivity in this zone was approximately 2 mm^2/s. However, the thermal diffusivities of both samples decreased with the increase of temperature when samples were aged at 220 °C and 240 °C. The thermal diffusivities of all of the samples reached similar values, then reduced with the increase of temperature in zone 3.

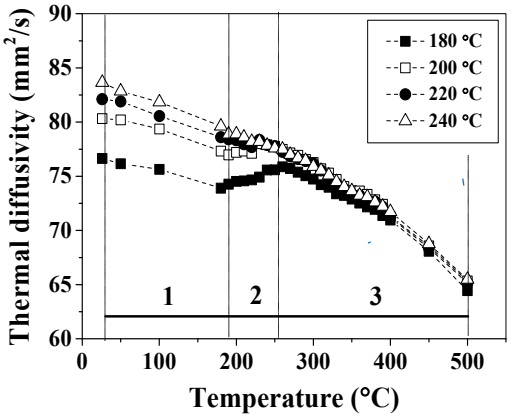

Figure 7. The thermal diffusivity changes of Al-1.1Mg_2Si samples according to the temperature increase with various contents and aging treatment conditions.

The aged Al-1.1Mg_2Si samples were investigated in terms of calorimetric analysis and shown in Figure 8.

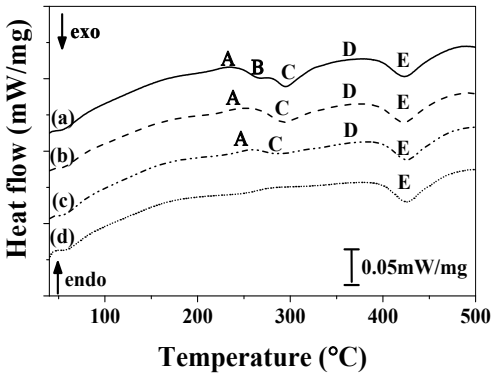

Figure 8. The heat flow curves of Al-1.1Mg2Si samples according to increase of aging treatment temperature: (**a**) 180 °C, (**b**) 200 °C, (**c**) 220 °C, and (**d**) 240 °C.

The exothermic peaks of A, B, and C were generated due to the precipitation reactions of β″, β′, and β, respectively, as mentioned earlier in Figure 3.

The exothermic reactions A, B, and C of the heat flow curve decreased with the increasing aging temperature. The area of the exothermic curve (enthalpy) indicates the number of precipitates generated during the calorimetric analysis [8]. Thus, the number of residual solutes decreased with the increasing aging temperature. The Al-1.1Mg_2Si specimen aged at 180 °C had the largest number of residual solutes, and the thermal diffusivity of this specimen was the lowest at 25 °C, as shown in Figure 7. However, in the case of the 240 °C aged sample, the precipitations of the β″ and β′ phases were nearly completed after the aging treatment. The precipitation reaction could not occur during the thermal diffusivity measurement in the 240 °C aged sample. The thermal diffusivity of this sample only decreased in zone 2, as shown in Figure 7.

The thermal diffusivity and the heat flow curves for the Al-3.5Mg_2Si aged specimens are shown in Figures 9 and 10. In Figure 9, the 180 °C aged sample had a nearly regular thermal diffusivity value of 62 mm^2/s in zone 1. The thermal diffusivity values at 25 °C increased with the increasing aging temperature.

The increment of the thermal diffusivity of the 180 °C aged specimen in zone 2 is 7 mm^2/s.

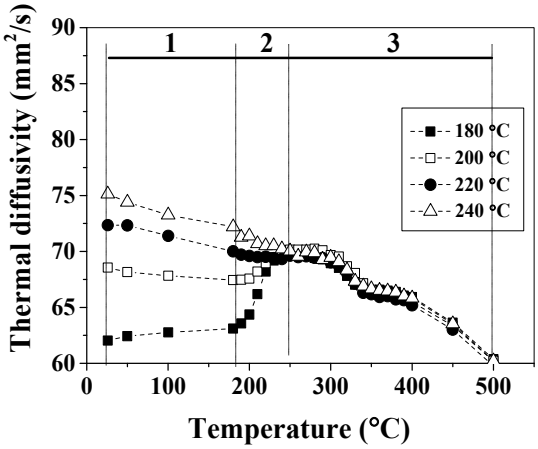

Figure 9. Thermal diffusivity changes of Al-3.5Mg_2Si samples according to the temperature increase with various contents and aging treatment conditions.

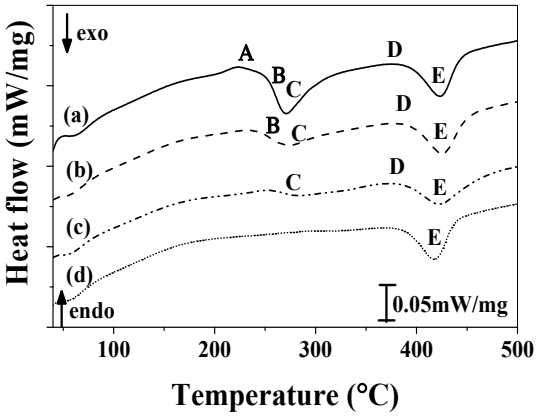

Figure 10. The heat flow curves of Al-3.5Mg_2Si samples according to increase of aging treatment temperature: (**a**) 180 °C, (**b**) 200 °C, (**c**) 220 °C, and (**d**) 240 °C.

The increment of 7 mm^2/s was larger than that of the Al-1.1Mg_2Si specimen aged in the same condition. The enthalpies of exothermic peaks A and B (precipitations of the β″ and β′ phases, respectively) were also larger, as seen in Figure 10, than those of the Al-1.1Mg_2Si sample (Figure 8). The thermal diffusivities of all of the alloys at the final temperature in zone 2 eventually became the same regardless of the aging treatment because the precipitation reactions of each alloy were completed at that temperature. The thermal diffusivities of all the specimens decreased with the increasing temperature in zone 3.

4. Conclusions

In this study, the effects of the precipitation of the Mg_2Si phase on thermal diffusivity were investigated according to the aging temperature of a binary Al-Mg_2Si specimen. The following conclusions were drawn:

1. The thermal diffusivity curves of the as-quenched and aged samples can be divided into three zones. The thermal diffusivity of the first zone is determined by the amount of residual solute after heat treatment and the additive content of alloys. The decreases of the residual solute increased thermal diffusivity at zone 1 after heat treatment. In addition, the Mg_2Si content increased with the decrease of thermal diffusivity.
2. Zone 2 can be changed by an additional aging treatment condition; this zone was also affected by solute atoms and their precipitation temperatures. The increment of thermal diffusivity strongly depended on the amounts of β″ and β′ precipitate in this zone. The aged samples at 240 °C had larger thermal diffusivity values than the others.
3. The temperature of the final zone was decided by the end temperature of Mg_2Si precipitation. In this zone, thermal diffusivity decreased with the increase in temperature because of solvent re-melting, lattice vibration, etc. Thermal diffusivity was affected by thermal content in this zone only. The aging condition did not affect the thermal diffusivity of zone 3.

Author Contributions: Conceptualization, Y.-M.K. and S.-W.C.; methodology, Y.-C.K. and S.-K.H.; formal analysis, Y.-M.K. and Y.-C.K.; investigation, Y.-M.K.; resources, Y.-M.K. and S.-K.H.; writing—original draft preparation, Y.-M.K.; writing—review and editing, S.-W.C. and S.-K.H.; project administration, C.-S.K.

Funding: This research received no external funding.

Acknowledgments: We gratefully acknowledge the support provided by the Ministry of Trade, Industry, and Energy (MTIE) of the Republic of Korea for funding our research program on the development of convergent manufacturing technology for IE4-class electric motors. The present research is part of the above-mentioned program.

Conflicts of Interest: The authors declare no conflicts of interest.

References

1. Keller, K.P. Cast heatsink design advantages. In Proceedings of the Sixth Intersociety Conference on Thermal and Thermomechanical Phenomena in Electronic Systems (ITHERM'98), Seattle, WA, USA, 27–30 May 1998; IEEE: Piscataway, NJ, USA, 1998; pp. 112–117.
2. Fok, S.C.; Shen, W.; Tan, F.L. Cooling of portable hand-held electronic devices using phase change materials in finned heat sinks. *Int. J. Therm. Sci.* **2010**, *49*, 109–117. [CrossRef]
3. Dorf, R.C. *The Electrical Engineering Handbook Series*; CRC Press: Boca Raton, FL, USA, 2003; ISBN 0849313333.
4. Mirkovich, V.V. Comparative method and choice of standards for thermal conductivity determinations. *J. Am. Ceram. Soc.* **1965**, *48*, 387–391. [CrossRef]
5. Tye, R.P. (Ed.) *Thermal Conductivity (Volumes 1, 2)*; Academic Press Inc.: New York, NY, USA, 1968; ISBN 9780127054018.
6. Donaldson, A.B.; Taylor, R.E. Thermal diffusivity measurement by a radial heat flow method. *J. Appl. Phys.* **1975**, *46*, 4584–4589. [CrossRef]
7. Parker, W.J.; Jenkins, R.J.; Butler, C.P.; Abbott, G.L. Flash method of determining thermal diffusivity. *J. Appl. Phys.* **1961**, *32*, 1679. [CrossRef]
8. Cheng, S.Z.D. *Handbook of Thermal Analysis and Calorimetry 3-Applications to Polymers and Plastics*; Elsevier: Amsterdam, The Netherlands, 2002; Volume 3, ISBN 0444512861.
9. Brown, M.E. *Introduction to Thermal Analysis: Techniques and Applications*; Springer Science & Business Media: Dordrecht, The Netherlands, 1988; Volume 1, ISBN 1402004729.
10. Tritt, T.M. *Thermal Conductivity: Theory, Properties and Applications*, 1st ed.; Kluwer Academic/Plemum Publishers: Dordrecht, The Netherlands, 2004; ISBN 0306483270.
11. Akoshima, M.; Baba, T. Study on a thermal-diffusivity standard for laser flash method measurements. *Int. J. Thermophys.* **2006**, *27*, 1189–1203. [CrossRef]
12. Ozturk, F.; Esener, E.; Toros, S.; Picu, C.R. Effects of aging parameters on formability of 6061-O alloy. *Mater. Des.* **2010**, *31*, 4847–4852. [CrossRef]
13. Gupta, A.K.; Lloyd, D.J.; Court, S.A. Precipitation hardening in Al-Mg-Si alloys with and without excess Si. *Mater. Sci. Eng. A* **2001**, *316*, 11–17. [CrossRef]
14. Caceres, C.H.; Davidson, C.J.; Wang, Q.G.; Griffiths, J.R. The effect of Mg on the microstructure and mechanical behavior of Al-Si-Mg casting alloys. *Metall. Mater. Trans. A* **1999**, *30*, 2611–2618. [CrossRef]
15. Doan, L.C.; Nakai, K.; Matsuura, Y.; Kobayashi, S.; Ohmori, Y. Effects of excess Mg and Si on the isothermal ageing behaviours in the Al-Mg2Si alloys. *Mater. Trans.* **2002**, *43*, 1371–1380. [CrossRef]
16. Davis, J.R. *Aluminum and Aluminum Alloys*; ASM International: Geauga County, OH, USA, 2006; ISBN 978-0-87170-496-2.
17. Gaber, A.; Gaffar, M.A.; Mostafa, M.S.; Zeid, E.F.A. Precipitation kinetics of Al-1.12 Mg2Si-0.35 Si and Al-1.07 Mg2Si-0.33 Cu alloys. *J. Alloys Compd.* **2007**, *429*, 167–175. [CrossRef]
18. Kim, Y.M.; Choi, S.W.; Hong, S.K. The behavior of thermal diffusivity change according to the heat treatment in Al-Si binary system. *J. Alloys Compd.* **2016**, *687*, 54–58. [CrossRef]
19. Choi, S.W.; Cho, H.S.; Kumai, S. Effect of the precipitation of secondary phases on the thermal diffusivity and thermal conductivity of Al-4.5Cu alloy. *J. Alloys Compd.* **2016**, *688*, 897–902. [CrossRef]
20. Edwards, G.A.; Stiller, K.; Dunlop, G.L.; Couper, M.J. The precipitation sequence in Al–Mg–Si alloys. *Acta Mater.* **1998**, *46*, 3893–3904. [CrossRef]
21. Daoudi, M.I.; Triki, A.; Redjaimia, A. DSC study of the kinetic parameters of the metastable phases formation during non-isothermal annealing of an Al-Si-Mg alloy. *J. Therm. Anal. Calorim.* **2011**, *104*, 627–633. [CrossRef]
22. Eskin, D.G.; Massardier, V.; Merle, P. Study of high-temperature precipitation in Al-Mg-Si alloys with an excess of silicon. *J. Mater. Sci.* **1999**, *34*, 811–820. [CrossRef]
23. Wahi, R.P.; von Heimendahl, M. On the occurrence of the metastable phase beta double prime in an Al-Si-Mg alloy. *Phys. Status Solidi Appl. Res.* **1974**, *24*, 607–612. [CrossRef]
24. Burger, G.B.; Gupta, A.K.; Jeffrey, P.W.; Lloyd, D.J. Microstructural control of aluminum sheet used in automotive applications. *Mater. Charact.* **1995**, *35*, 23–39. [CrossRef]
25. Zhang, J.; Fan, Z.; Wang, Y.Q.; Zhou, B.L. Microstructural development of Al–15wt.%Mg2Si in situ composite with mischmetal addition. *J. Mater. Sci. Eng.* **2000**, *281*, 104–112. [CrossRef]

26. Hatch, J.E.; Association, A.; Metals, A.S. *Aluminum: Properties and Physical Metallurgy*; Aluminum/J.E. Hatch [Hrsg.]; American Society for Metals: Geauga County, OH, USA, 1984; ISBN 9780871701763.
27. Tritt, T.M. (Ed.) *Thermal Conductivity: Theory, Properties, and Applications*; Kluwer Academic/Plenum: New York, NY, USA, 2004; ISBN 0306483270.
28. Shackelford, J. *Introduction to Materials Science for Engineers*; Pearson Prentice Hall: Upper Saddle River, NJ, USA, 1988; ISBN 9780136012603.
29. Brown, M.; Gallagher, P. *Handbook of Thermal Analysis and Calorimetry, Volume 5 Recent Advances, Techniques and Applications*; Elsevier: Amsterdam, The Netherlands, 2008; Volume 5, ISBN 9780444531230.